Analele Universităţii de Vest din Timişoara
Vol. XLIX, 2006
Seria Fizică

SEMI-ACTIVE DAMPER WITH MAGNETORHEOLOGICAL SUSPENSION

Gheorghe Catana

Department of Physics. West University of Timisoara, Bd. V. Parvan, No. 4, 1900 Timisoara. ROMANIA

Abstract

The semi-active damper with magnetorheological suspension is made up of a cylinder with piston. There is an outer interchangeable nozzle between the cylinder compartments. The magnetic field created in the nozzle, by an electromagnet, changes the viscosity of the magnetorheological suspension (particles average diameter: 2.14 μm; volumetric fraction: 11.5%). A traction test machine has highlighted the traction – compression force as function of the magnetic field intensity (max. 68kA·m^{-1}) for piston driving speeds (6mm/min, 10mm/min, and 220 mm/min) and nozzle diameters of 0.9mm and 1.9 mm. The force multiplication coefficient, under the presence of the magnetic field, does not depend on the nozzle diameter. Its maximum value is 20, for piston driving speeds of 6 mm/min., and for magnetic field intensities of 68 kA·m^{-1}.

Keywords: Damper, Magnetorheological suspension, Iron micro particles, Magnetic field, Traction test machine.

1. Introduction

Magnetorheological suspension (MRS) dampers are devices with which the dynamic viscosity of the fluid is altered by an external magnetic field.

There have been created dampers [1] with MRS for commercial purposes. Studies are being developed for the use of dampers in aviation [2], for the protection against earthquakes of the civil and industrial buildings [3], etc.

There are studies of large interest in [4-6] that deal with modeling the operation of dampers with MRS.

Following all these research works, there has been found out that MRS dampers cannot be made for any type of application. Consequently, various constructive and functional options of MRS dampers have been proposed. Thus, [1] presents a damper with which the MRS is retained by an absorbing material (polystyrene), while [5] describes a damper with piston-coil and internal hydraulic channels, and finally, [7] presents a damper with internal hydraulic circuit and external coil.

Following up this research direction, the paper presents below a semi-active damper with MRS, as well as the experimental results that have been obtained on a traction test machine.

2. Experimental device

The semi-active damper with MRS (Fig. 1) is made up of the following components: cylinder 1, piston 2 with spindle 3, and the hydraulic circuit 4.

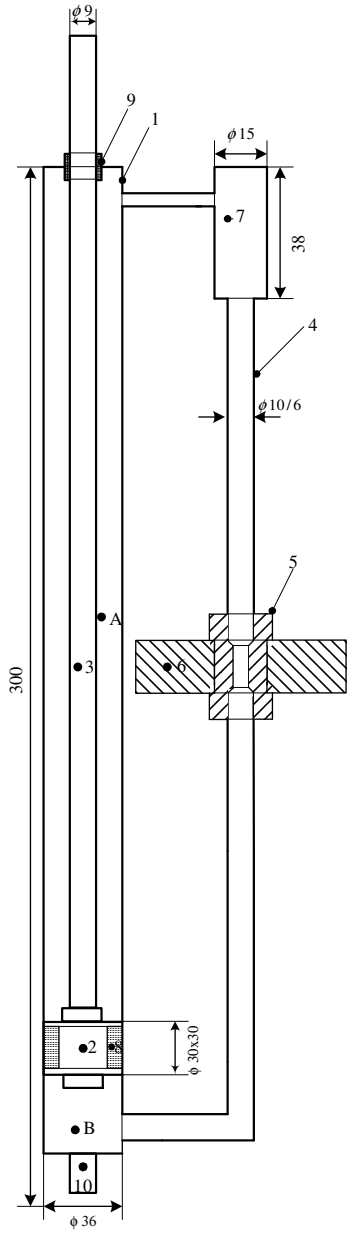

Fig. 1 – Semi-active damper with MRS (schematic diagram): 1 – cylinder, 2 – piston, 3 – spindle, 4 – external hydraulic circuit; 5 – nozzle, 6 – electromagnet, 7 – volume compensating chamber, 8 – tightening gasket, 9 – spindle tightening block, 10 – fixing screw – damper positioning, A and B – compartments.

Cylinder 1 is provided with the compartments A and B limited by piston 2. The MRS is driven, from one compartment to the other, by piston 2. In both cases, the MRS travels through nozzle 5. The nozzle (Fig. 2) has the length “l” and diameter “d”. It is placed between the poles of electromagnet 6 (Fig. 3), and is interchangeable.

Chamber 7 is meant for the damper supply with MRS, and for compensating the suspension volume displaced by spindle 3. The particles form chains in the nozzle channel under the effect of the magnetic field [8]. Thus, the suspension is transformed into a viscous-plastic body [9, 10].

The change of the suspension viscosity, as function of the magnetic field intensity, leads to the change of speeds and stress in the fluid medium.

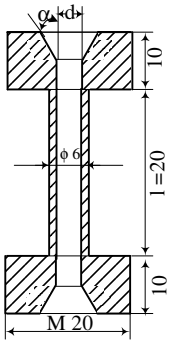

Fig. 2 – Nozzle: d – diameter, l – channel length, $\alpha \sim 10°$ – nozzle concinnity;

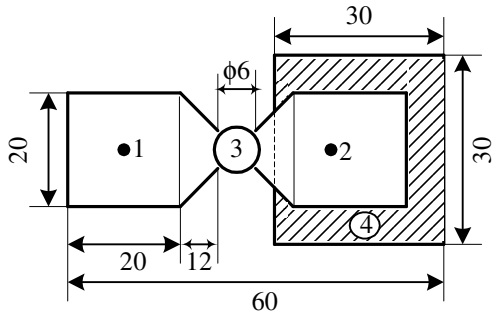

Fig. 3 – Electromagnet and nozzle (cross section) 1 and 2 – electromagnet poles, 3 – nozzle channel, 4 – coil;

2. Model

The nozzle channel in Fig. 2 is situated in a homogeneous magnetic field. The MRS travels uniformly (Fig. 4).

The traveling speeds of the suspension are small (~ x 10^{-3}m·s^{-1}, and the suspension temperature is always constant.

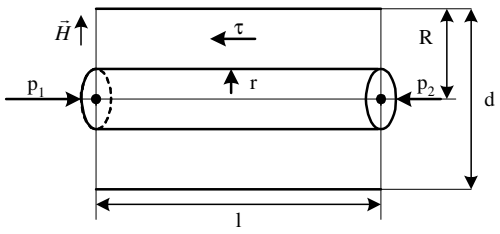

Fig. 4 – Model for the study of the forces equilibrium on some cylinder of "r" radius, formed in the MRS under the influence of an external magnetic field of "H" intensity;

On a section of finite length "l", within the travelling range $r \in [0, R]$, the pressure forces equilibrium $(p_1 - p_2)\cdot\pi\cdot r^2$ (the flow driving force), and the viscosity forces equilibrium $2\pi\cdot r\cdot l\cdot\tau_n$ are made (they hinder the suspension travel): $2\pi\cdot r\cdot l\cdot\tau_n = (p_1 - p_2)\cdot\pi\cdot r^2$ wherefrom there results the tangential unitary effort:

$$\tau_n = \frac{r(p_1 - p_2)}{2l} = \frac{r\Delta p_n}{2l} \qquad (1)$$

The suspension within the magnetic field is a viscous-plastic body. Consequently, the expression of the tangential unitary effort, given by Bingham, will be entered in relation (1). In case of the circular pipe on the right, it becomes: $\tau_n = \tau_0 - \eta_n \frac{dv_n}{dr}$. There results the following: $\tau_0 - \eta_n \frac{dv_n}{dr} = \frac{r\Delta p_n}{2l}$, a differential equation with separable variables, through the integration of which the following solution will be obtained:

$$v_n = \frac{\tau_0}{\eta_n}\cdot r - \frac{r^2}{4l\cdot\eta_n}\cdot\Delta p_n + C_1 \qquad (2)$$

The integration constant C_1 is obtained out of the adhesion condition of the suspension on the solid surface (for r = R there results $v_n = 0$). The following is obtained:

$$C_1 = \frac{R^2}{4l\cdot\eta_n}\cdot\Delta p_n - \frac{\tau_0}{\eta_n}R$$

which if entered into (2) leads to:

$$v_n = \frac{R^2 - r^2}{4l\cdot\eta_n}\cdot\Delta p_n - \frac{R - r}{\eta_n}\cdot\tau_0 \qquad (3)$$

where η_n is the dynamical viscosity, and τ_0 is the threshold stress of the MRS.

Expression (3) represents the law of variation of the suspension speed in the circular pipe. It is of parabolic type (Fig. 5), with the maximum speed in the pipe axis. For r = 0, there results:

$$v_{n\,max} = \frac{R}{\eta_n}\left(\frac{R\cdot\Delta p_n}{4l} - \tau_0\right) \qquad (4)$$

For $\Delta p_n > 4l\tau_0/R$, relation (4) has a fixed direction, and if $\Delta p_n < 4l\tau_0/R$, the travel is no longer possible.

The tangential unitary effort, given by relation (1) expresses a linear distribution (Fig. 5), identical with that obtained during Hagen – Poiseuille travel. For r = R, there is obtained $\tau_p = \tau_{max} = 0.5\,\Delta p_n R$ and consequently: $\tau_n/\tau_p = r/R$.

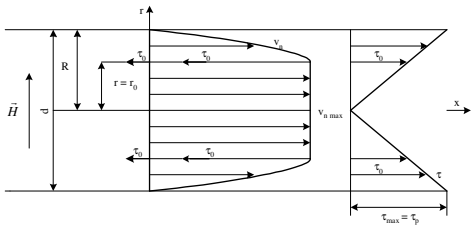

Fig. 5 – The distribution of tangential speeds v_n and efforts τ in the cross section of a cylindrical pipe of "R" radius, that is placed in a magnetic field of "H" intensity, through which a MRS travels freely;

Since in the central zone, i.e. for $r \in [0, r_0]$, there is no shearing ($\tau_n < \tau_0$), there results that the suspension travels as if it is a solid body .

The flow will be calculated by dividing the transversal cross section of the pipe in the two flowing ranges, and the total flow will be:

$$Q_n = Q_{n0} + Q_{n1} = \pi r_0^2 v_{no} + \int_{r_0}^{R} 2\pi r\, v_n dr \qquad (5)$$

where v_{no} is obtained from (3) for $r = r_o$ and $\tau_0 = \Delta p_n r_0/2l$, under the form of:

$$v_{no} = \frac{\Delta p_n}{4l\eta_n}(R^2 - r_0^2) - \frac{\tau_0}{\eta_n}(R - r_0) = \frac{\Delta p_n}{4l\eta_n}(R - r_0)^2 \qquad (6)$$

Expressions (3) and (6) will be entered into (5), and after their integration, since $R > r_0$ there results:

$$Q_n = \frac{\pi\Delta p_n R^4}{8l\eta_n}\left[1 - \frac{4}{3}\left(\frac{r_0}{R}\right)\right] \qquad (7)$$

The average travelling speed of the suspension in the pipe cross section is given by the following ratio:

$$v_{n\,m} = \frac{Q_n}{\pi R^2}\frac{\Delta p_n R^2}{8l\eta_n} = \left(1 - \frac{4}{3}\frac{r_0}{R}\right) \qquad (8)$$

which for $\tau_0/\tau_p = r_0/R$ results under the form of:

$$v_{n\,m} = \frac{\Delta p_n}{8l\eta_n}\left(1 - \frac{4}{3}\frac{\tau_0}{\tau_p}\right) \qquad (8')$$

The threshold stress τ_0 depends on the intensity H of the magnetic field [11], thus:

- for $H < H_{sat}$: $$\tau_0 = \sqrt{6}\ \varphi \mu_0\ M_s^{\frac{1}{2}}\ H^{\frac{3}{2}} \qquad (9)$$

- for $H \geq H_{sat}$: $$\tau_0^{sat} = 86 \cdot 10^{-3}\ \varphi \mu_0\ M_s^2 \qquad (10)$$

where H_{sat} is the intensity of the magnetic field corresponding to the saturation magnetization M_S of the particles, φ is the volumic fraction of the solid phase of the suspension, and μ_0 is the magnetic permeability of the vacuum.

If relations (9) and (10) are entered into (8'), the following is obtained:

$$v_{n\,m} = \frac{\Delta p_n}{8 l \eta_n}(1 - 37.97\ H^{\frac{3}{2}} \cdot\ M_s^{-\frac{3}{2}}) \qquad (11)$$

For:

$$H_c = 0.08851\ M_s \qquad (12)$$

there results from (11) that $v_{n\,m} = 0$.

The pressure variation Δ_p for H = 0 is maintained by applying force F_o to the piston (Fig. 1), and then out of (8') there results the following:

$$\Delta p = \frac{F_0}{S} = \frac{8 v_m \eta l}{R^2} \qquad (13)$$

The presence of the magnetic field, alters the suspension viscosity, from η to η_n and then out of (11) their results the following:

$$\Delta p_n = \frac{F}{S} = \frac{8 v_{nm} \eta_n l}{R^2 (1 - 37.97 H^{\frac{3}{2}} M_s^{-\frac{3}{2}})} \qquad (14)$$

where $S = \pi R^2$ is the area of the piston transversal cross section (Fig. 1).

In case $v_m = v_{n\,m}$, F_o shall be multiplied, i.e.:

$$. \square = \frac{F}{F_0} = \frac{\eta_n}{\eta}\ \frac{1}{1 - 37.97 H^{\frac{3}{2}} M_s^{-\frac{3}{2}}} \qquad (15)$$

3. Experimental results and discussions

The accomplished damper has the assembly configuration presented in Fig. 1. The brass nozzle (Fig. 2) has the following diameters: d_1 = 0.9 mm and d_2 = 1.9 mm. The electromagnet configuration and dimensions are presented in Fig. 3. The magnetic field generated by the electromagnet has intensities of max. 68 kA/m (Fig. 6).

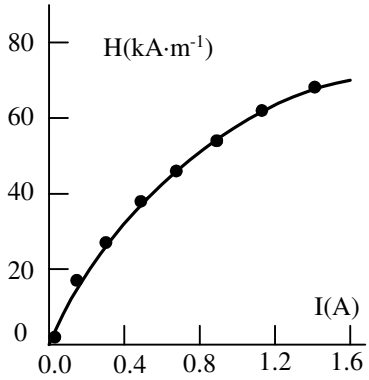

Fig. 6 – The variation of "H" intensity of the magnetic field as function of "I" intensity of the electric current through the electromagnet coil;

The MRS [12], having the volume of 65 cm^3 ± 5 %, is based on siliconic oil, stearic acid and iron particles. The volumic fraction of the solid component is of 11.5%. The magnetic particles have the average diameter of 2.10 μm, for a standard deviation of σ = 0.42 μm (Fig. 7). The damper is tested on a traction test machine. The piston driving speeds are as follows:

- step I: 6 mm. $min.^{-1}$ ± 2.5 %;
- step II: 10 mm.$min.^{-1}$ ± 2.5 %;
- step III: 220 mm.$min.^{-1}$ ± 2.0 %.

Within the 0–200 N ± 1.5 % range there have been measured forces F_o for the piston driving, in the absence of the magnetic field, and forces F for the piston driving, in the presence of the magnetic field, respectively.

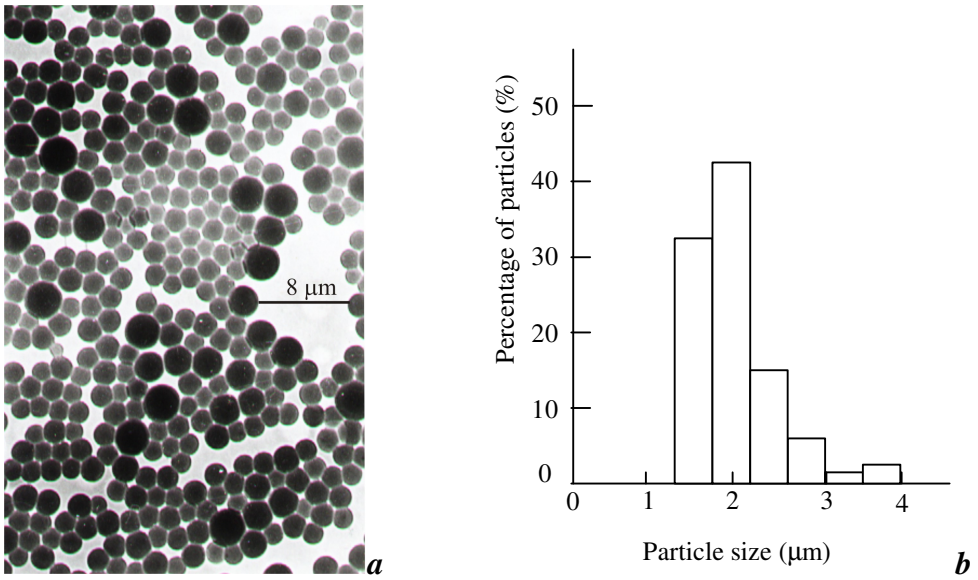

Fig. 7 – Iron particles: Forms and dimensions (a), Particle size distribution (b)

The dependence of force F on the current intensity through the coil for the piston driving speed and nozzle diameter, as parameter, is shown in Fig. 8. The rate of curves is the same. But, F values depend on the intensity of the current through the coil, on the nozzle diameter, and on the piston driving speed. The maximum force is F = 60 N for the nozzle diameter of 0.9 mm, and the piston driving speed of 220 mm · min^{-1}.

The dependence of □ = F/F_0 quantity on the intensity "I" of the current through the coil, for piston driving speeds and nozzle diameters is shown in Fig. 9.

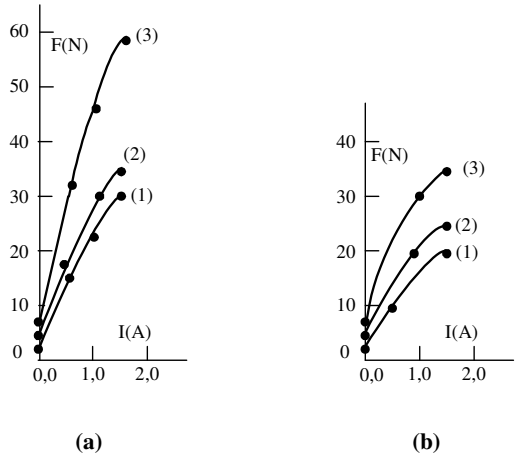

Fig. 8 – The variation of F (N) piston driving force as function of "I (A)" intensity of the electric current through the coil for: - nozzle diameter: (a) d_1 = 0.9 mm; (b) d_2 = 1.9 mm; - piston driving speeds: (1) 6 mm · min^{-1}; (2) 10 mm · min^{-1}; (3) 220 mm · $min^{-1;}$

It can be seen in Fig. 9 that β quantity does not depend on the nozzle diameter. But β depends on the piston driving speed and on the intensity of the electric current through the coil. Its maximum value (β=20) is for I =1.5Ad.c. and the piston driving speed of 6mm.·min^{-1}.

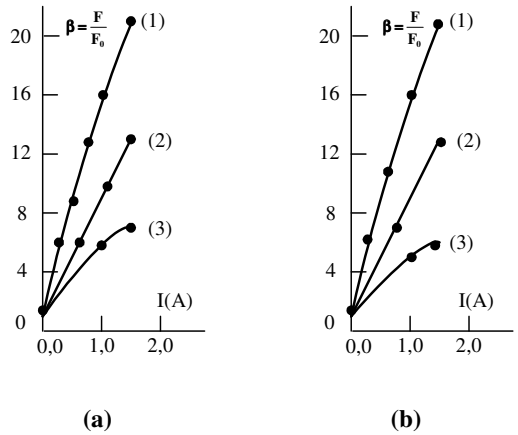

Fig. 9 – The variation of $\beta = F/F_o$ as function of "I (A)" intensity of the electric current through the coil, for: - nozzle diameter (a) d_1 = 0.9 mm; (b) d_2 = 1.9 mm; - piston driving speeds: (1) 6 mm · min^{-1}; (2) 10 mm · min^{-1}; (3) 220 mm · min^{-1};

Out of expression (13) there can be obtained the expression of η quantity under the following form:

$$\eta = \frac{F_0}{8\pi v_m l}\left(\frac{R}{R_p}\right)^2 \qquad (16)$$

Values between 87 Pa·s and 768 Pa·s result for the dynamic viscosity of the suspension (Table 1).

Crt. No	d (mm)	v_m (mm/min)	F_0 (N)	η (Pa·s)
1	00.9	6	1.5	210
2		10	3.0	252
3.		220	8.0	31
4.	11.9	6	1	640
5.		10	2	768
6.		220	5	87

Since force F_o is meant for the uniformly driving of the piston, there results from Table 1 that η depends on the diameter d = 2R of the nozzle, and on the piston driving speed, v_m, respectively. The dimension η_n/η, as function of the magnetic field intensity H, results from expression (15), under the following form: $\frac{\eta_n}{\eta} = (1 - 37.97\ H^{\frac{3}{2}} \cdot M_s^{-\frac{3}{2}}) \cdot$ □ (17)

For β values in Fig. 9, and corresponding H values, respectively, (Fig. 6), there can be obtained, out of (17), the variation of η_n/η as function of the intensity "I" of the electric current through the coil (Fig. 10).

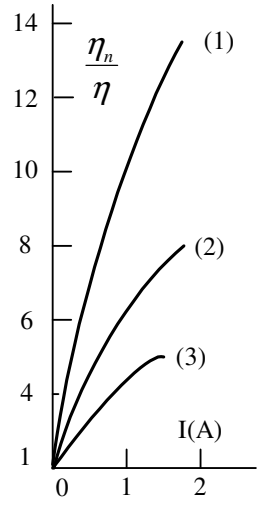

Fig. 10 – The variation of η_n/η. quantity as function of "I (A)" intensity of the electric current through the coil, for: (1) 6 mm · min^{-1}; (2) 10 mm · min^{-1}; (3) 220 mm · min^{-1};

It can be observed out of Fig. 10 that η_n/η quantity depends only on the electric current intensity "I" through the coil, and on the piston driving speed v_m, respectively. Out of

Table 1 and Fig. 10 there can be obtained the variation of dynamic viscosity, η_n, as function of the electric current intensity "I" for v_m piston driving speeds, and "d" diameters of the nozzle (Fig. 11).

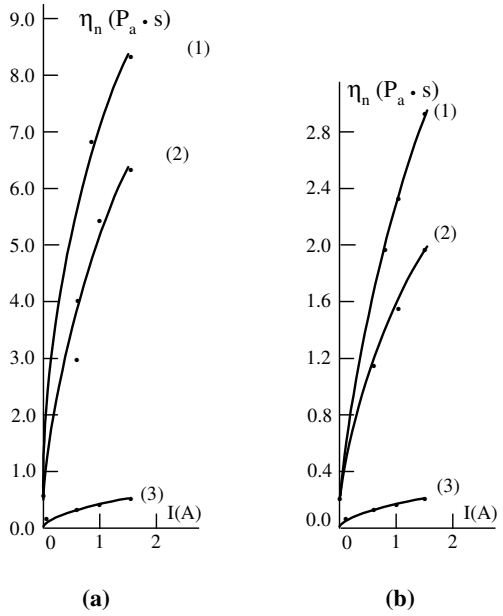

Fig. 11 – The variation of η_n viscosity of the MRS as function of "I (A)" intensity of the electric current through the coil, for: - nozzle diameter: (a) 1.9 mm; (b) 0.9 mm; - piston driving speeds: (1) 6 mm · min^{-1}; (2) 10 mm · min^{-1}; (3) 220 mm · min^{-1}.

It can be observed that η_n depends on the piston driving speed, and on the electric current intensity through the coil. With the speed increase v_m, and the nozzle diameter decrease, η_n decreases. The minimum value is of 110 Pa·s for the piston speed of 220 m · min^{-1} and electric current intensities through the coil of 1.5A d.c. (Fig. 11 b). It can be seen from Fig. 11 that the variation of the MRS viscosity η_n, as function of the intensity "I" of the electric current through the coil implies a similar modification of F, forces with the uniform movement of the suspension through the nozzle (Fig. 8). The dynamic viscosity η_n of the suspension in the magnetic field increases 13.4 times; compared with the dynamic viscosity of the same suspension, but if the magnetic field is absent (Fig. 10).

4. Conclusions

The accomplished damper, as per the diagram in Fig. 1, is reliable and robust. As far as the MRS based on siliconic oil, stearic acid and iron particles (average diameter: 2.10 μm, volumic fraction: 11.5%) is concerned: the piston driving force at speeds of 6 mm · min^{-1} with

the presence of the magnetic field (68 kA/m) increases with up to 20 times, compared with the piston driving force, with the absence of the external magnetic field (Fig. 9);

• the piston driving force has a quasilinear variation with the electric current intensity through the coil (Fig. 8);

• the dynamic viscosity of the suspension alters with the increase of the electric current intensity "I(A)" through the coil (Fig. 11);

• report η_n/η reaches values of max. 13.4 for I = 1.5A d.c. and $v_m = 6$ mm · min^{-1} (Fig. 10);

We consider that the damper in Fig. 1 can be used with:

• hydraulic control circuits;

• equipments meant for the characterization of the MRS and for studying the damper function;

• vibrations damper systems and for mechanical shocks absorption.

References

[1] J.D. Carlson, In "Proced. of the 7th Int. Conf. on ERF and MRS" (edited by R. Tao, World Scientific Publishing, Singapore, 1999), 621–628.

[2] V.Madhavan, G.M. Kamatah, N.M. Wereley, In "Proced. of the 7th Int. Conf. on ERF and MRS" (edited by R. Tao, World Scientific Publishing, Singapore, 1999), 639–647.

[3] G.M. Hiemenez, N.M. Wereley, In "Proced. of the 7th Int. Conf. on ERF and MRS" (edited by R. Tao, World Scientific Publishing, Singapore, 1999), 657–664.

[4] W.H. Liao, C.Y. Lay, Smart Mat. Struct. **11** (2002), 288–296.

[5] G.Y. Zhou, P.Q. Zhang, Smart Mat. Struct. **11** (2002), 230–238.

[6] W.H. Li, H. Du, G. Chen, S.H. Yeo, N.Q. Guo, Smart Mat. Struct. **11** (2002), 209–217.

[7] I. Bica, J. Magn. Magn, Mater. **241** (2002), 196–20l.

[8] X. Wang, F. Gordaninejad, In "Proced. of the 7th Int. Conf. on ERF and MRS" (edited by R. Tao, World Scientific Publishing, Singapore, 1999), 568–578.

[9] D.–Y. Lee, N.M. Wereley, In "Proced. of the 7th Int. Conf. on ERF and MRS" (edited by R. Tao, World Scientific Publishing, Singapore, 1999), 579–586.

[10] W.Korodonski, S. Gorodkin, N. Zhuranski, In "Proced. of the 7th Int. Conf. on ERF and MRS" (edited by R. Tao, World Scientific Publishing, Singapore, 1999), 611–620.

[11] J.M. Ginder, L.C. Davis, L.D. Elie, Int. J. Mod. Phys. **B 10** (1996), 3293–3296

[12] I. Bica, Mat. Sci. Eng. B – in press